Optimal Load Distribution of Transporting System for Large Flat Panel Displays

Jong Won Kim* , Jang Gun Jo* , Hyun Chan Cho* , Doo Yong Kim**

* School of Information Technology at Korea University of Technology and Education,

** Division of Information Technology at Soonchunhyang University

ABSTRACT

This paper proposes an intelligent method for the optimal load distribution of two cooperating robots(TCRs) using fuzzy logic. The proposed scheme requires the knowledge of the robots' dynamics, which in turn depend upon the characteristics of large flat panel displays(LFPDs) carried by the TCRs. However, the dynamic properties of the LFPD are not known exactly, so that the dynamics of the robots, and hence the required joint torque, must be calculated for nominal set of the LFPD characteristics. The force of the TCRs is an important factor in carrying the LFPD. It is divided into external force and internal force. In general, the effects of the internal force of the TCRs are not considered in performing the load distribution in terms of optimal time, but they are essential in optimal trajectory planning; if they are not taken into consideration, the optimal scheme is no longer fitting. To alleviate this deficiency, we present an algorithm for finding the internal-force factors for the TCRs in terms of optimal time. The effectiveness of the proposed system is demonstrated by computer simulations using two three-joint planner robot manipulators.

Key Words : Two cooperating robots; fuzzy logic; intelligent load distribution; large flat panel displays

1. INTRODUCTION

In recent years, multi-robot systems have been paid attention to semiconductors and displays manufacturing industry. It is important that robots should safely transfer large flat panel displays(LFPDs) to next manufacturing stations. As a size of LFPDs increases it may not be adequate for using a single robot for transportation systems. If a single robot carries a LFPD it could damage the surface of the LFPD due to the unbalanced force. In order to overcome the drawback of a single robot transportation system, multi-robot systems should be considered. It is certain that we can increase the productivity and safety employing multi-robot systems.

But, it is a challenging problem to coordinate multiple robots in terms of time delays, system reliability and flexibility, and controllability.

Until now many researchers have investigated the optimal load distribution problem considering mechanical stress minimization, jerk minimization, energy minimization, and else for the TCRs. But the effects of internal forces on the TCRs have not been considered in performing the load distribution in terms of optimal time. The effect of internal forces on the optimal path planning is essential. If they are not taken into consideration

the optimal scheme is no longer fitting.
Unfortunately, it is very hard to determine these factors for the optimal path planning. This is primarily due to the fact that they do not have a unique numerical solution. Moreover, enormous computation time will be required, even if they can be determined by a certain method. To overcome such difficulties, we employ some concepts of fuzzy logic. Fuzzy logic enables us to formulate an intelligent algorithm emulating human reasoning in making a decision to obtain the optimal solution to this problem[1-3].
The problem of the TCRs is more complicated, when compared with the use of a single robot(manipulator), because it involves some complicated kinematic and dynamic constrains during the cooperating motion.
In this paper, the kinematic relations (of position, velocity and acceleration) between the two robots are established. Then, the new parametric dynamic equations will be obtained, including the internal forces between the LFPD and the two robots, which are determined by fuzzy logic.

2. KINEMATIC RELATIONS

2.1. Specification of Positions

It is assumed that a Cartesian path is given in terms of the center of mass of the LFPD, which the TCRs are supposed to grasp and carry (figure 1). The path of the LFPD, $\mathbf{X}_o(s)$ in $\Re^6$, can be represented as

$$\mathbf{X}_o(s) = [\mathbf{P}_o(s)\mathbf{R}_o(s)]^T \tag{1}$$

where $s(o \le s \le s_f)$ is a normalized distance parameter[4], $\mathbf{P}_0(s) \in \Re^3$ denotes a position vector, and $\mathbf{R}_0(s) \in \Re^3$ is a orientation vector expressed in the Euler-angle representation.
When the LFPD moves along the given path, the relative positions ($\mathbf{P}_{oi} \in \Re^3$, $i=1,2$) and orientations ($\mathbf{R}_{oi} \in \Re^3$, $i=1,2$) of the TCRs must be constant with respect to the center of mass of the LFPD (figure 1). Accordingly, the path $\mathbf{X}_i(s) \in \Re^6$, of the i-th ($i=1,2$) robot manipulator can be represented as

$$\mathbf{X}_i(s) = [\mathbf{P}_i(s) \quad \mathbf{R}_i(s)^T] \tag{2}$$

$$\mathbf{P}_i(s) = \mathbf{P}_o(s) + {}^B_o\mathbf{R}_o(s) \cdot \mathbf{P}_{oi} \tag{3}$$

$$\mathbf{R}_i(s) = [\delta \mathbf{x}_i(s), \delta \mathbf{y}_i(s), \delta \mathbf{z}_i(s)] \tag{4}$$

where ${}^B_o\mathbf{R}_o(s) \in \Re^{3X3}$ denotes the rotation of the LFPD with respect to the base coordinate, $\mathbf{P}_i(s) \in \Re^3$ and $\mathbf{R}_i(s) \in \Re^3$ (which is determined by ${}^B_0\mathbf{R}_0(s) \cdot \mathbf{P}_{0i}$), are the position vector and the orientation vector expressed in the Euler-angle of the i-th manipulator, respectively[5].
When the TCRs move along the paths specified by (2), (3) and (4), the LFPD obviously moves along the given geometric Cartesian path. Therefore, we may focus on the TCRs paths rather than on the path of the LFPD.

2.2. Determining Velocity and Acceleration

The Cartesian velocity $\dot{\mathbf{X}}_i(s)$ and the acceleration $\ddot{\mathbf{X}}_i(s)$ of the i-th manipulator (i=1,2) are simply obtained by the chain rule as follows:

$$\dot{\mathbf{X}}_i(s) = \frac{d\mathbf{X}_i(s)}{ds}\dot{s} \tag{5}$$

$$\ddot{\mathbf{X}}_i(s) = \frac{d\mathbf{X}_i(s)}{ds}\dot{s} + \frac{d^2\mathbf{X}_i(s)}{ds^2}\dot{s}^2 \tag{6}$$

The Cartesian velocity given by (5) is usually related to the corresponding joint velocities by the formula

$$\dot{\mathbf{X}}_i(s) = \mathbf{J}(\boldsymbol{\theta}_i(s))\dot{\boldsymbol{\theta}}_i(s) \ (i=1,2) \tag{7}$$

where $\theta \in \Re^6$ is a generalized joint position vector of the i-th manipulator and $\mathbf{J}(\cdot) \in \Re^{6\times 6}$ denotes the corresponding Jacobian matrix. In the following, the symbols in $\theta_i(s)$ and $\dot{\theta}_i(s)$ is omitted for the sake of simplicity. Utilizing (7), the Cartesian acceleration of the i-th manipulator can be determined as

$$\ddot{\mathbf{X}}_i(s) = \dot{\mathbf{J}}(\theta_i,\dot{\theta}_i)\cdot\dot{\theta}_i + \mathbf{J}(\theta_i)\cdot\ddot{\theta}_i \ (i=1,2) \tag{8}$$

Thus, the joint acceleration $\ddot{\theta}_i(s) \in \Re^6$ of the i-th manipulator is related to the Cartesian velocity by the equation

$$\ddot{\theta}_i(s) \equiv \phi_1^i(s)\ddot{s} + \left[\phi_2^i(s) + \phi_3^i(s)\right]\dot{s}^2 \quad (i=1,2) \tag{9}$$

where $\phi_j(s) \in \Re^6 (j=1,2,3)$ is defined by substituting (6) and (7) into (8) as follows:

$$\phi_1^i(s) \equiv \mathbf{J}^{-1}(\theta_i)\frac{d\mathbf{X}_i(s)}{ds} \tag{10}$$

$$\phi_2^i(s) \equiv \mathbf{J}^{-1}(\theta_i)\frac{d^2\mathbf{X}_i(s)}{ds^2} \tag{11}$$

$$\phi_3^i(s) \equiv -\mathbf{J}^{-1}(\theta_i)\frac{d\mathbf{J}_i(\theta_i)}{ds}\mathbf{J}^{-1}(\theta_i)\frac{d\mathbf{X}_i(s)}{ds} \quad (i=1,2) \tag{12}$$

3. DYNAMIC RELATIONS

3.1. Parameterization of the Dynamic Equations

The dynamic characteristics of the manipulator are highly nonlinear and coupled. The

Lagrangian formulation for a six-joint manipulator is described by the formula[6]

$$\mathbf{U}_j = \sum_{k=1}^{6} \mathbf{D}_{jk}(\theta)\ddot{\theta}_k + \sum_{k=1}^{6}\sum_{l=1}^{6} \mathbf{C}_{jkl}(\theta)\dot{\theta}_k\dot{\theta}_l + \sum_{k=1}^{6} \mathbf{R}_{jk}\dot{\theta}_k + \mathbf{g}_j(\theta) \quad (j=1,2,\cdots,6) \tag{13}$$

where $\mathbf{U}_j$ is the input torque applied at joint j, $\mathbf{D}_{jk}(\theta)$ is the inertia term between joints j and k, $\mathbf{C}_{jkl}(\theta)$ is the Coriolis effect at joint j due to the velocity of joints k and l (for $l=k$, centrifugal force due to the velocity of joint k), $\mathbf{R}_{jk}$ is the friction term, and $\mathbf{g}_j(\theta)$ denotes the gravity effect.

With the assumption that the two manipulators have the same dynamic characteristics, substituting the joint velocities(from (7)) and the joint accelerations given by (9) into the dynamic formula (13) yields the parametric equations

$$\mathbf{U}_j^i(s) = \mathbf{M}_j^i(s)\ddot{s} + \mathbf{Q}_j^i(s)\dot{s}^2 + \mathbf{R}_j^i(s)\dot{s} + \mathbf{G}_j^i(s) \quad (i=1,2 \text{ and } j=1,2,\cdots,6) \tag{14}$$

where

$$\mathbf{M}_j^i = \sum_{k=1}^{6} \mathbf{D}_{jk}^i(\theta_i)\ \phi_{1k}^i(s)$$

$$\mathbf{Q}_j^i = \sum_{k=1}^{6} \mathbf{D}_{jk}^i(\theta_i)\left[\phi_{2k}^i(s) + \phi_{3k}^i(s)\right] + \sum_{k=1}^{6}\sum_{l=1}^{6} \mathbf{C}_{jkl}^i(\theta_i)\ \phi_{1k}^i(s)\phi_{1l}^i(s)$$

$$\mathbf{R}_j^i = \sum_{k=1}^{6} \mathbf{R}_{jk}^i\ \phi_{1k}^i(s)$$

$\mathbf{G}_j^i = \mathbf{g}_j^i(\theta_i)$ and $\phi_{jk}^i(s)(j=1,2,3)$ is the k-th element of the vector $\phi_j^i(s)$.

3.2. Internal Forces

During the cooperating movement of the two manipulators, there exists an important issue to be taken into consideration. It is the relationship of internal forces between the LFPD and the TCRs . In general, the LFPD moving along the given path has the force and moment vector $\mathbf{F}_0(s) \in \Re^6$ described by the formula

$$\mathbf{F}_0(s) = \begin{bmatrix} \mathbf{f}_0(s) - m\mathbf{g}^0 \\ \mathbf{n}_0(s) \end{bmatrix} = \begin{bmatrix} m\dfrac{d\mathbf{P}^0(s)}{ds} \\ \mathbf{D}^0\dfrac{d\mathbf{R}^0(s)}{ds} \end{bmatrix}\ddot{s} + \begin{bmatrix} m\dfrac{d^2\mathbf{P}^0(s)}{ds^2} + \mathbf{D}^0\dfrac{d^2\mathbf{R}^0(s)}{ds} + \dfrac{d\mathbf{R}^0(s)}{ds} \times \dfrac{d\mathbf{R}^0(s)}{ds} \end{bmatrix}\dot{s}^2 + \begin{bmatrix} m\mathbf{g}^0 \\ 0 \end{bmatrix} \tag{15}$$

where $\mathbf{f}_0(s) \in \Re^3$ and $\mathbf{n}_0(s) \in \Re^3$ are, respectively, the linear force and moment vectors of the moving LFPD, m, $\mathbf{D}_0 \in \Re^{3\times3}$, $\mathbf{g}_0(s) \in \Re^3$ are, respectively, the mass, the inertia matrix and the gravity term of the LFPD, and ' $\times$ ' denotes the vector cross product.

In order for the LFPD to move along the specified trajectory, the force and the moment vector $\mathbf{F}_0(s)$ must be supplied by both manipulators. Thus, if the total force and moment

vector to be applied at the LFPD by the TCRs are denoted by $\mathbf{F}_i(s)\in\Re^6$, $\mathbf{F}_i(s)$ and $\mathbf{F}_0(s)$ must satisfy the equation

$$\mathbf{F}_0(s)=\mathbf{W}\cdot[\mathbf{F}_1(s)\ \ \mathbf{F}_2(s)]=\mathbf{W}\cdot[\mathbf{f}_1(s)\ \ \mathbf{n}_1(s)\ \ \mathbf{f}_2(s)\ \ \mathbf{n}_2(s)] \tag{16}$$

where $\mathbf{f}_i(s)=[\mathbf{f}_{ik}(s)]\in\Re^3$ and $\mathbf{n}_i(s)=[\mathbf{n}_{ik}(s)]\in\Re^3$ $(i=1,2\ and\ k=x,y,z)$ denote distributed force vectors applied to the LFPD by the i-th manipulator, respectively, and $\mathbf{W}\in\Re^{6\times12}$ defined by (17), is a constant transformation matrix including the kinematic relationship between each end-effector of the TCRs and the center of mass of the LFPD(figure 2). The distributed forces for each manipulator are determined by a pseudo-inverse matrix via the equation Barnett[3]

$$[\mathbf{F}_1(s)\ \ \mathbf{F}_2(s)]^T=\mathbf{W}^+\mathbf{F}_0(s)+(\mathbf{I}-\mathbf{W}^+\mathbf{W})\xi \tag{17}$$

where $\mathbf{W}^+\mathbf{F}_0(s)=\mathbf{W}^T(\mathbf{W}^+\mathbf{W})^{-1}\cdot\mathbf{F}_0(s)$ is the force carrying the LFPD, $(\mathbf{I}-\mathbf{W}^+\mathbf{W})\zeta$ is the internal force vector that does not have any effect on the moving LFPD, and $\zeta=[\zeta_1,\zeta_2,\cdots,\zeta_v]\in\Re^{12}$ is an unknown arbitrary vector

In order for each manipulator to get the distributed force, we redefine (17) as follows:

$$\mathbf{W}^+=[\ (\mathbf{W}_1^+)^T\ (\mathbf{W}_2^+)^T\cdots(\mathbf{W}_n^+)^T\ ]^T \tag{18}$$

$$\mathbf{I}-\mathbf{W}^+\mathbf{W}=[\ (\mathbf{I}-\mathbf{W}^+\mathbf{W})_1\ (\mathbf{I}-\mathbf{W}^+\mathbf{W})_2\cdots(\mathbf{I}-\mathbf{W}^+\mathbf{W})_n\ ]^T \tag{19}$$

Hence, the distributed force can be expressed as

$$\mathbf{F}(s)=\mathbf{W}_n^+\cdot\mathbf{F}_0(s)+(\mathbf{I}-\mathbf{W}^+\mathbf{W})_n\cdot\zeta \tag{20}$$

Finally, if determining ζ from (17) in terms of optimal time, a dynamic equation of the considered internal forces will be obtained:

$$\begin{aligned}\mathbf{U}_j^i(s)&=\mathbf{M}_j^i(s)\ddot{s}+\mathbf{Q}_j^i(s)\dot{s}^2+\mathbf{R}_j^i(s)\dot{s}+\mathbf{G}_j^i(s)+\mathbf{J}_j^{iT}\mathbf{F}(s)\\&\equiv\hat{\mathbf{M}}_j^i(s)\ddot{s}+\hat{\mathbf{Q}}_j^i(s)\dot{s}^2+\hat{\mathbf{R}}_j^i(s)\dot{s}+\hat{\mathbf{G}}_j^i(s)\ \ (i=1,2\ and\ j=1,2,\cdots,6),\end{aligned} \tag{21}$$

4. DETERMINATION OF THE MAXIMUM BOUNDARY CURVE BY FUZZY-OPTIMAL LOAD DISTRIBUTION

The first term on the right-hand side of (17) represents forces that are supplied by the manipulators to carry the LFPD. The second term, which does not involve the moving LFPD, represents internal forces, which offset each other.

As maximum allowable input torques' boundary of the manipulator is decreased or increased by internal forces, the maximum velocity for time-optimal path planning is decreased or

increased, respectively. A maximum velocities and accelerators of robots should be determined within torque limits. The allowable torque boundary is decreased in proportion to increase load and the speed of robot should be decreased. So If the amount of load for each robot is able to be controlled, especially in case of cooperating robot systems, we can obtain the load distribution and more speed of TCRs and obtain new velocity curve in phase plane and new switching points of acceleration and deceleration. If the area of velocity curve is larger than before, the switching points should be located higher point. Therefore, the selection of ζ for optimal load distribution is an important issue in terms of optimal time planning for the TCRs.

Unfortunately, it is very difficult to obtain ζ by mathematical methods because of heavy computation. So it is useful to determine it by an intelligent algorithm based on fuzzy logic.

4.1. Construction of the Maximum Boundary Curves of Each Manipulator

Using (21), which describes the dynamics of the i-th manipulator(including the internal force when ζ =0)[7-11], the input torque can be represented by that of acceleration as follows:

$$-{}^{i}\mathbf{U}_j^{\max} - \mu_j^i(s,\dot{s}) \le \hat{\mathbf{M}}_j^i(s)\ddot{s} \le {}^{i}\mathbf{U}_j^{\max} - \mu_j^i(s,\dot{s}) \ (\mathrm{i}=1,2 \text{ and } \mathrm{j}=1,2,\ldots,6) \tag{22}$$

where $\mu_j^i(s,\dot{s}) \equiv \hat{\mathbf{Q}}_j^i(s)\,\dot{s}^2 + \hat{\mathbf{R}}_j^i(s)\dot{s} + \hat{\mathbf{G}}(s)$.

If $\overline{\mathbf{M}_j^i}(s) \neq 0$ ($i=1,2$ *and* $j=1,2,\ldots,6$), the admissible range of the acceleration $\ddot{s}$ at each point s, which can be derived from (22), is expressed by the inequalities

$$\mathbf{L}_j^i(s,\dot{s}) \le \ddot{s} \le \mathbf{H}_j^i(s,\dot{s}) \quad (\mathrm{i}=1,2 \text{ and } \mathrm{j}=1,2,\ldots,6) \tag{23}$$

where

$$\mathbf{L}_j^i(s,\dot{s}) = \begin{cases} \left|\hat{\mathbf{M}}_j^i(s)\right|^{-1}\left[-{}^{i}\mathbf{U}_j^{\max} - \mu_j^i(s,\dot{s})\right], & \hat{\mathbf{M}}_j^i(s) > 0 \\ \left|\hat{\mathbf{M}}_j^i(s)\right|^{-1}\left[{}^{i}\mathbf{U}_j^{\max} - \mu_j^i(s,\dot{s})\right], & \hat{\mathbf{M}}_j^i(s) < 0 \end{cases}$$

$$\mathbf{H}_j^i(s,\dot{s}) = \begin{cases} \left|\hat{\mathbf{M}}_j^i(s)\right|^{-1}\left[{}^{i}\mathbf{U}_j^{\max} - \mu_j^i(s,\dot{s})\right], & \hat{\mathbf{M}}_j^i(s) > 0 \\ \left|\hat{\mathbf{M}}_j^i(s)\right|^{-1}\left[-{}^{i}\mathbf{U}_j^{\max} - \mu_j^i(s,\dot{s})\right], & \hat{\mathbf{M}}_j^i(s) < 0. \end{cases}$$

From (23), an the important restriction can be obtained so that TCRs can move along the given paths within the bounded input torques. This restriction is expressed by the inequality

$$\mathbf{H}_j^i(s,\dot{s}) - \mathbf{L}_j^i(s,\dot{s}) \ge 0 \quad (\mathrm{i}=1,2 \text{ and } \mathrm{j},\mathrm{k}=1,2,\ldots,6). \tag{24}$$

Applying (24) to all the joints of the two manipulators, the range of commonly admissible velocity and the maximum velocity boundary at each point can easily be determined.

4.2. Background for Fuzzy Optimal Load Distribution

As an example, figure 3 shows the maximum velocity boundary curves for each manipulator, without considering the internal force in case of $\zeta=0$ and the commonly admissible boundary curve(LBC; Lower Boundary Curve).

The maximum velocity profile of the TCRs should be just under LBC area. In figure 3, the LBC area is the intersection area of the two maximum velocity boundary curves($=\dot{s}^1_{max} \cap \dot{s}^2_{max}$) in the whole s area. That is, the maximum velocity profile for the TCRs is restricted by the lower of two manipulators. If the LBC' s area is increased, the maximum velocity profile of the TCRs could be changed toward higher speed.

Although the two maximum velocity boundary curves are the same, the velocities of each manipulator are not the same. There is a switching point between the maximum velocity boundary curves of each manipulator, as shown in figure 3. When s is placed at this point, ζ need not to be selected by using fuzzy logic, because each robot manipulator has the same maximum velocity boundary. If ζ is optimally selected by fuzzy logic, LBC of the TCRs increases and becomes similar to the average curve in figure 3.

Figure 4 shows the position and orientation of the LFPD when the two robots carry a LFPD. P_o is the center point of the LFPD in figure 4. P_1 is the contact point of the manipulator # 1 in figure 4. P_2 is the contact point of the manipulator # 2 in figure 4. The elevation difference has an effect on the load of the TCRs. In order for the TCRs to optimize this scheme using fuzzy rules, they consist of two inputs (difference of kinematic data and maximum velocity boundary) and one output (vector ζ).

4.3. Determination of Fuzzy Rules

We propose appropriate fuzzy rules to find the optimal ζ . They are based on two kinds of information about difference between each maximum boundary curve of the TCRs and about static properties of the LFPD path velocity.

Each manipulator has a different load according to the difference of the position, the orientation and the path of the LFPD in Cartesian space. Fuzzy rules are composed of two kinds. Rules of the first kind reflect the static properties and the characters of the relations between the LFPD and each manipulator. These rules select ζ . A single rule of the second kind is a velocity curve rule, which decreases or increases the difference between two maximum bound velocities for each manipulator and selects ζ .

4.3.1. Fuzzy Rules Based on Static Properties

Fuzzy rules involving static properties are constructed according to the difference of

position, orientations and the path of the LFPD and the TCRs . As the path of each manipulator depends on the path of the LFPD, these rules are constructed in terms of the acceleration and deceleration directions of the LFPD path. At first, we only thought the mass gravity problems. The difference of mass gravity for each manipulator depends on the difference of altitude of each position(P_0 , P_1 , P_2)of the LFPD(in figure 4). The difference of the altitude between the P_1 and P_2 in figure 4 is chosen as one input in the fuzzy inference rules, because the difference of load for each manipulator is directly proportional to the difference of altitude. The second input in the rules is the difference of the maximum boundary curve ($e = \dot{s}^1_{\max} \cap \dot{s}^2_{\max}$), because the dynamic equations of the two manipulators are only parameterized by s and $\dot{s}$. The relation between the forces and the elements of ζ which are the consequent part of the fuzzy rules is given by (20). Forces in (20) are composed of $f_{ik} \in f_i$ and $n_{ik} \in n_i$ (i=1,2 and k=x,y,z) . If P_1 locates a lower position than P_2 , manipulator #1 may be loaded more than manipulator #2. Moreover, if two manipulators have different maximum boundary curves in spite of the same dynamic characteristics, then there must be many constraints(different payloads, different paths, etc.) for the two manipulator. This fact that one has a small maximum velocity boundary curve may be the fact that it has a heavier load than the other. We use a fuzzy rule to enable each manipulator to have same allowable velocity boundary curves.

When $\dot{s}^1_{\max} - \dot{s}^2_{\max} \geq 0$ and $P_{1y} - P_{2y} \geq 0$, the position of contact point for the manipulator #1 must be at a higher position than the position of contact point for the manipulator #2 and must have a less load because $\dot{s}^1_{\max} - \dot{s}^2_{\max} \geq 0$ in spite of same dynamics. The force vector is composed of two factors(external, internal force) in (20). ζ , the element of the internal force, is an arbitrary vector and will be selected by fuzzy logic in order to adjust the distributed force between the LFPDs and each manipulator. The adjusted force enables the maximum velocity boundary of each manipulator to increase or decrease.

All elements of $\zeta \in \Re^{12}$ obtained by fuzzy logic, adjust the payload of each manipulator and make it possible to get the optimal load distribution. It is not easy to find the optimal fuzzy rule. So the velocity rule will be added for selecting the optimal ζ with e and $\dot{e}$ in order to decrease the error. Figure 5 shows a block diagram for fuzzy logic. All elements of ζ are obtained by adding ζ of fuzzy static rule and $\Delta\zeta$ of fuzzy velocity rule for optimal load distribution.

4.3.2 Velocity Boundary Curve Rule

The static fuzzy rule depends upon kinematic data of manipulators and the LFPD. Kinematic data may be fixed at any position along the predefined path. ζ obtained by static fuzzy rule may not contribute to minimizing the difference of boundary curves, because the inputs of static fuzzy rule are kinematic data and kinematic data are fixed along the path Velocity boundary curve rule based on dynamics should be needed for moving the LFPD along

the path with time-optimal path planning. We must set the optimal ζ in order to minimize the difference of maximum boundary curves. ζ vector is the element of internal force term and is contributed to the dynamics of robot. The maximum boundary curves of TCRs will be changed by adjusting ζ to minimize the difference. The velocity boundary curve rule is based on the error descent method. It produces $\Delta\zeta$ (figure 5). An example of this fuzzy rule is: If e is B and $\dot{e}$ is F then $\Delta\zeta$ is G , where e is the difference between the maximum boundary curve of $\dot{s}_1$ and the maximum boundary curve of $\dot{s}_2$, $\dot{e}$ is de/ds. B, F and G are fuzzy sets representing states of the fuzzy variables, respectively

4.4. Fuzzy-Optimal Load Distribution

The method for optimal load distribution of the TCRs using fuzzy logic can be expressed in terms of the following algorithm.

Fuzzy-optimal load distribution

Step 1. Establish the relationship of position and orientation between the TCRs and the LFPD.

Step 2. $\dot{s}_i=0$

Step 3. If $\dot{s}_i=s_f\ (i=0,1,\cdots,f)$, then stop this algorithm.

Step 4. Evaluate (16) of the LFPD.

Step 5. Evaluate (17) ($\mathbf{F}(s)=\mathbf{W}^{+}\mathbf{F}_0(s)+(\mathbf{I}-\mathbf{W}^{+}\mathbf{W})\zeta$) using outcomes of Step 1 and Step 4.

Step 6. Evaluate (21) under the assumption that $\zeta=0$.

Step 7. Construct the maximum boundary curves(MBC) of each manipulator by (24).

Step 8. If the maximum boundary curves of each manipulator are the same ($e=\dot{s}_1^{max}-\dot{s}_2^{max}=0$), then they define the optimal boundary curves for the TCRs . Go to Step 3 after replacing s_i with s_{i+1}. Else, go to the next step.

Step 9. Select the static fuzzy rule according to e and the position difference.

Step 10. Select the velocity fuzzy rule according to e and $\dot{e}$.

Step 11. Determine vector ζ for optimal load distribution by fuzzy inference using the Max-Min method and the Center of Gravity method.

Step 12. Construct (21). Go to Step 7.

The proposed method had been simulated by using two planar manipulators each with three joints, as shown in figure 6. The moving path of the LFPD on Cartesian space is selected as

$$x = r_0 ,$$
$$y = r_0 + s ,$$
$$\theta_0 = (\frac{\pi}{4}) \cdot s \qquad (25)$$

where r_0 is a constant value, sampling rate of s is 0.001, and θ_0 rotates with respect to axis Z from 0° to 45°. Each manipulator links' length and mass are shown in the table 1.
Figure 7 shows the construction of the boundary curves with considered optimal load distribution of the internal forces by fuzzy logic when the optimal load distribution is considered. Fuzzy rules for obtaining ζ_1 and ζ_7 are shown in figure 8, as examples

5. CONCLUSIONS

The optimal load distribution of the TCRs becomes an important issue in many industrial applications(such as transfer, assembly, etc.). However, such an optimal load distribution is more difficult than that of the single case. In this paper, an intelligent approach is proposed to solve the problem effectively. At first, the kinematic/dynamic relations between a LFPD and two manipulators during the cooperating motion are closely investigated In particular, the optimal load distribution using fuzzy logic in terms of optimal time is established without any mathematical method.
The effectiveness of the proposed intelligent load distribution was demonstrated by a computer simulation. This approach can be easily expanded to the case of multiple (more than two)cooperative robot manipulators or finger robot.
Also, the proposed method could be applicable for deriving the path trajectory in terms of optimal time.

References

1. Klir, G. J. and Yuan, B. (1995), *Fuzzy sets and Fuzzy Logic*, Prentice Hall, Upper Saddle River, NJ.

2. Zimmermann, H. J. (1985), *Fuzzy Set Theory and Its Applications*, Kluwer-Nijho., Boston.

3. Barnett, S. (1971), *Matrices in Control Theory*, VanNorst and Reinhold, New York.

4. Fox, E. A. (1967), *Mechanics*, Harper and Publishers

5. Craig, J. J. (1989), *Introduction to Robotics: Mechanics and Control*, Addison-Wesley.

6. Paul, R. P. (1982), *Robot Manipulators: Mathematics, Programming and Control*, The MIT Press

Cambridge, Mass.

7. Cho, H. C., Jeon, H. T. and Lee, H. G. (1990), " Generation of optimal-time trajectory for the two cooperating robot manipulators." *1990 IEEE Int. Conf. on Systems, Man and Cybernetics* , LA, 457-462.

8. Takagi , T. and Sugeno, M. (1985), " Fuzzy identification of systems and its applications to modeling and control." *IEEE Transactions Systems, Man and Cybernetics*, 15 , 116-132.

9. Yoshikawa , T. and Zheng, X-Z (1993), " Coordinated Dynamic Hybrid Position/Force Control of Multiple Robot Manipulators Handling One Constrained LFPDs." *International Journal on Robotics Research*, 12(3), 219-229.

10. Zheng , Y. F. and Luh, J. Y. S. (1988), " Optimal Load Distribution for Two Industrial Robot Handling a Single LFPDs." *IEEE Conference on Robotics and Automation*, 344-349.

11. Zadeh, L. A. (1965), Fuzzy sets, *International Control*, 8, 338-353.

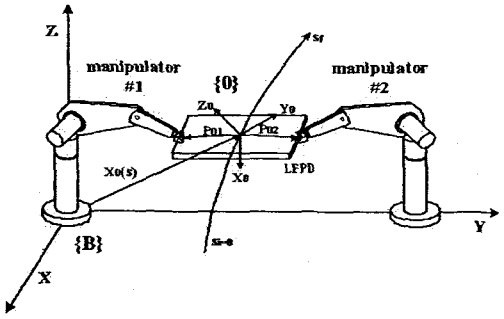

Fig. 1 Cooperating motion of the TCRs grasping a solid LFPD

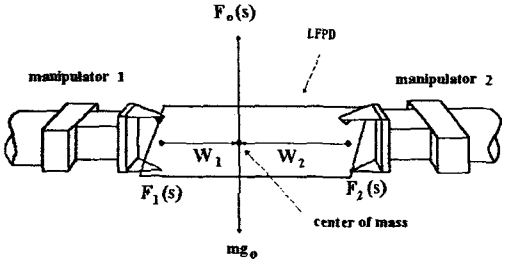

Fig. 2 Transformation of the force and moments between the LFPD and the TCRs

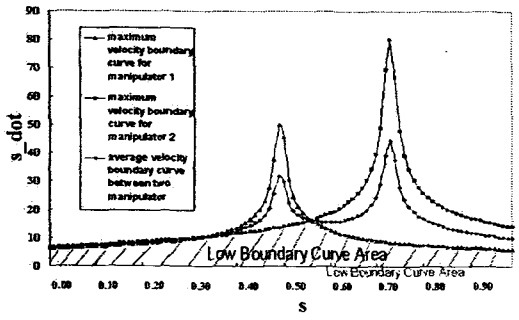

Fig. 3 Maximum velocity boundary curve

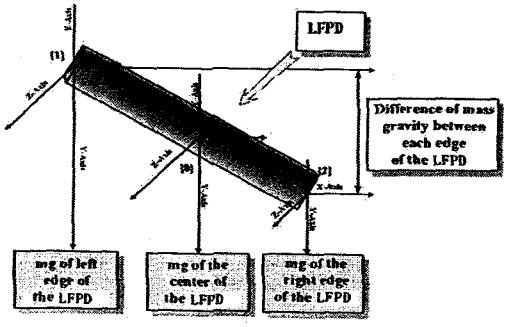

Fig. 4 Concept for the load distribution

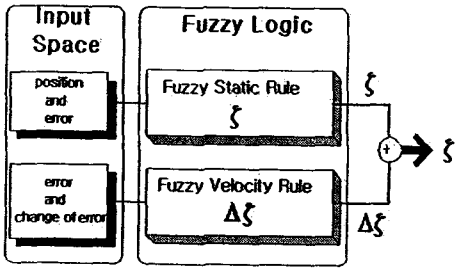

Fig. 5 Fuzzy logic block diagram

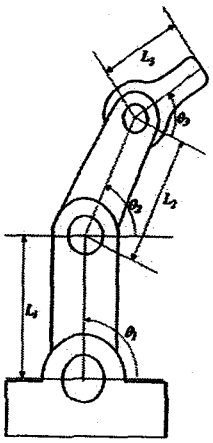

Fig. 6 3-d.o.f. planar robot manipulator

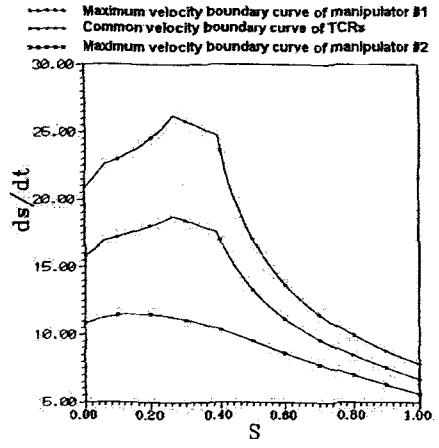

Fig. 7 Common velocity boundary curve obtained by fuzzy logic

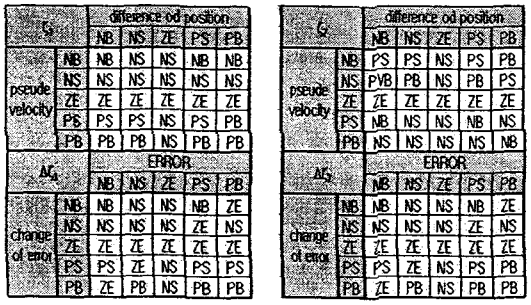

ζ_1		difference od position				
		NB	NS	ZE	PS	PB
pseude velocity	NB	NB	NS	NS	NB	NB
	NS	NS	NS	NS	NS	NS
	ZE	ZE	ZE	ZE	ZE	ZE
	PS	PS	PS	NS	PS	PB
	PB	PB	PB	NS	PB	PB
$\Delta\zeta_1$		ERROR				
		NB	NS	ZE	PS	PB
change of error	NB	NB	NS	NS	NB	ZE
	NS	NS	NS	NS	ZE	NS
	ZE	ZE	ZE	ZE	ZE	ZE
	PS	PS	ZE	NS	PS	PS
	PB	ZE	PB	NS	PB	PB

ζ_2		difference od position				
		NB	NS	ZE	PS	PB
pseude velocity	NB	PS	PS	NS	PS	PB
	NS	PVB	PB	NS	PB	PS
	ZE	ZE	ZE	ZE	ZE	ZE
	PS	NB	NS	NS	NB	NS
	PB	NS	NS	NS	NS	NB
$\Delta\zeta_2$		ERROR				
		NB	NS	ZE	PS	PB
change of error	NB	NB	NS	NS	NB	ZE
	NS	NS	NS	NS	ZE	NS
	ZE	ZE	ZE	ZE	ZE	ZE
	PS	PS	ZE	NS	PS	PB
	PB	ZE	PB	NS	PB	PB

Fig. 8 Fuzzy rules for obtaining ζ_1 and ζ_2

Table 1. The link parameters of the 3-d.o.f. robot manipulator

PRIVATE	LINK 1	LINK 2	LINK 3
Length	1.6 m	1.4 m	0.25m
Mass	7 kg	5 kg	3kg